
Effect of Internal Convection and Internal Radiation on the Structural Temperatures of Space Shuttle Orbiter

William L. Ko, Robert D. Quinn, and Leslie Gong
Ames Research Center, Dryden Flight Research Facility, Edwards, California

1988



National Aeronautics and
Space Administration

Ames Research Center

Dryden Flight Research Facility
Edwards, California 93523-5000

CONTENTS

SUMMARY	1
NOMENCLATURE	1
INTRODUCTION	2
DESCRIPTION OF PROBLEM	3
INTERNAL CONVECTION	3
Fuselage	3
Wing	3
FREE CONVECTIVE HEAT TRANSFER COEFFICIENTS	4
Vertical Surfaces	4
Horizontal Surfaces	4
RESULTS	5
Fuselage	5
Wing	5
CONCLUSIONS	5
APPENDIX—THERMAL PROPERTIES OF SPACE SHUTTLE ORBITER MATERIALS	7
REFERENCES	13
TABLES	13

PRECEDING PAGE BLANK NOT FILMED

SUMMARY

Structural performance and resizing (SPAR) finite-element thermal analysis computer program was used in the reentry heat transfer analysis of the space shuttle orbiter. One midfuselage cross section and one midspan wing segment were selected to study the effects of internal convection and internal radiation on the structural temperatures. The effect of internal convection was found to be more prominent than that of internal radiation in the orbiter thermal analysis. Without these two effects, the calculated structural temperatures at certain stations could be as much as 45 to 90 percent higher than the measured values. By considering internal convection as free convection, the correlation between the predicted and measured structural temperatures could be improved greatly.

NOMENCLATURE

C_p	specific heat, Btu/lb-°F
C_i	correlation parameters in free convection equation
C21	two-node convection element
HRSI	high-temperature reusable surface insulation
FRSI	felt reusable surface insulation
F_{ij}	radiation view factor from element i to element j
g	acceleration due to gravity, in./sec ²
h	free convection heat transfer coefficient, Btu/in. ² -sec-°F
i	integers, 1, 2, 3, ...
JLOC	joint location (or node)
j	integers, 1, 2, 3, ...
K21	two-node conduction element
K31	three-node conduction element
K41	four-node conduction element
k	conductivity, Btu/ft-hr-°F or Btu/in.-sec-°F
L	length, in.
LRSI	low-temperature reusable surface insulation
p	pressure, lb/ft ²
R21	two-node radiation element
RTV	room temperature vulcanized
SIP	strain isolation pad
r	reflectivity
SPAR	structural performance and resizing
STS-5	space transportation system 5
T	temperature, °F or °R

TC	thermocouple
TPS	thermal protection system
T_g	bulk temperature of gas, °R
T_w	average wall temperature, °R
t	time, sec
X_0	station on the x axis
x, y, z	rectangular Cartesian coordinates
Y_0	station on the y axis
γ	weight density, lb/in. ³ or lb/ft ³
ϵ	emissivity
μ	viscosity, lbm/in.-sec
ρ	density, lb/ft ³

INTRODUCTION

In past reentry heat transfer analysis of the space shuttle orbiter (Gong and others, 1984; Gong and others, 1982; Ko and others, 1981, 1982, 1986), the effect of internal convection was neglected because it was assumed that the effect of internal convection was secondary as compared with the effects of conduction and internal and external radiations. The results of the past analysis showed excellent agreement between the calculated and measured thermal protection system (TPS) surface temperatures over the entire reentry time span, including the period after touchdown (Ko and others, 1986, 1987). However, the calculated and measured substructural temperatures of the fuselage and the wing lower skins agreed nicely only until the time immediately before touchdown (Ko and others, 1986, 1987). The agreement broke down after touchdown, and the measured substructural temperatures consistently showed lower values. It was revealed by the manufacturer of the orbiter that air vents at the orbiter wing roots were usually opened to allow the external air to enter the orbiter interior to eliminate the danger of collapsing the orbiter when it descended to denser air environment (at $t = 1400$ sec, or 100,000 ft altitude). The air ingested into the orbiter would definitely result in internal free convection cooling and may possibly result in forced convection cooling. It was felt (based upon the results of the measured structural temperatures) that the major mode of heat transfer was free convection. Consequently, to improve the agreement between measured and calculated structural temperatures, a thermal analysis was made with the inclusion of internal free convection (Ko and others, 1987).

The results of this analysis showed that the agreement was improved but was still not satisfactory. This indicated that the ingested air resulted in mostly forced convective heat transfer rather than free convective heat transfer as previously thought. Therefore, an analysis was made with internal forced convection (Ko and others, 1987). Since the air velocities in the wing bays were unknown, it was necessary to make estimates of the velocities. The velocities were estimated so that the resulting heat transfer coefficients were sufficient to produce the required cooling and bring the calculated temperature into good agreement with the measured data. However, it has subsequently been discovered that there are errors in the free convection code of the structural performance and resizing (SPAR) thermal analyzer computer program. These errors caused the calculated free convection heat transfer coefficients to be much lower than the true values. With this new information, it became most probable that the major mode of internal convective heat transfer was free convection as initially deduced.

The purpose of this report is to calculate orbiter fuselage structural temperatures and recalculate the orbiter wing structural temperatures using correctly calculated internal free convection heat transfer coefficients, and to compare

the calculated results with measured temperatures. We also compare the relative intensities of the effects of internal free convection and internal radiation on the structural temperatures of the orbiter.

DESCRIPTION OF PROBLEM

The locations of midfuselage cross section FS877 and the midspan wing segment WS240 selected for the reentry heat transfer analysis are shown in figure 1. The reentry heating rates are based on the space transportation system 5 (STS-5) flight trajectory shown in figure 2. The existing SPAR thermal models set up for FS877 and WS240 are shown, respectively, in figures 3 and 4 (Gong and other, 1984; Gong and others, 1982; Ko and others, 1981, 1982, 1986, 1987). Based on the STS-5 surface heating rates shown, respectively, in figures 5 and 6 for FS877 and WS240, and the thermal properties shown in the appendix, the previously calculated TPS surface temperatures agreed nicely with the flight-measured temperatures from the beginning of reentry ($t = 0$), until after rollout (figs. 7 and 8). However, the calculated and the measured substructural temperatures compared very well from the reentry time ($t = 0$) up to $t = 1700$ sec, and after that the agreement broke down if the internal convection effect was neglected. The finite element solutions overpredicted the structural temperatures after $t = 1700$ sec (figs. 9 and 10). Since most of the convective cooling effect occurred after touchdown and rollout when the ingested air has lost its flow velocities, the internal convection is free convection rather than forced convection. The problem is to use the SPAR program, with the corrected internal free convection heat transfer coefficients, to calculate (or recalculate) the structural temperatures of FS877 and WS240 and also to compare the relative magnitudes of the effects of internal free convection and internal radiation on the orbiter structural temperatures.

INTERNAL CONVECTION

Fuselage

Normally the effects of free convection would be accounted for by introducing five-node free convection (C53) elements in the SPAR program (Marlowe and others, 1979). The program would then compute the free convection heat transfer coefficient and the corresponding convective heat transfer. However, because of the shape of the fuselage cross section, the SPAR program could not handle the free convection calculations. Therefore, internal free convection in FS877 was simulated by using the two-node forced convection (C21) elements and calculating the heat transfer coefficients for these elements by using the free convection heat transfer equations found in the SPAR program. In figure 11, we show 96 C21 elements attached to the inner surfaces of the cargo bay and the glove of the existing fuselage thermal model FS877 (fig. 3) to model the internal convection.

Wing

The bays of the wing model WS240 have distinct sharp corners and the five-node free convection SPAR elements (C53) can be used to account for free convection heat transfer. However, as mentioned in the Introduction section, there are errors in the free convection code of the SPAR program which result in the computation of erroneous free convection heat transfer coefficients. Therefore, free convective heat transfer was included in the wing analysis by using four-node forced convection (C41) elements and calculating heat transfer coefficients by using the free convection equations that are in the SPAR program. These hand-calculated free convection heat transfer coefficients were input to the SPAR program by data set CONV PROP. In this way, the error in the free convection computer code was circumvented, and the effects of free convection heat transfer were simulated by using C41 elements. In figure 12, we show 88 C41 elements set up for WS240 four-bay cavities.

FREE CONVECTIVE HEAT TRANSFER COEFFICIENTS

The internal heat transfer coefficient h (Btu/in.²-sec-°F) were calculated from the following equation for free convection:

$$\frac{hL}{k} = C_1 G_r^{C_2} P_r^{C_3} \quad (1)$$

where

$$G_r \equiv g \frac{\rho^2}{\mu^2} L^3 \Delta T \beta \quad (2)$$

$$P_r \equiv \frac{C_p \mu}{k} \quad (3)$$

C_i ($i = 1, 2, 3$) = correlation parameters

g = acceleration due to gravity, in./sec²

ρ = density lb/in.³

μ = viscosity, lbm/in.-sec

L = side length, in.

C_p = specific heat, Btu/lb-°F

k = conductivity, Btu/in.-sec-°F

T_g = bulk temperature of gas, °R

T_w = average wall temperature, °R

$\beta = 2/(T_g + T_w)$

$\Delta T = |T_g - T_w|$, °F

The properties are evaluated at the average of the gas and sidewall temperatures. The values of the correlation parameters C_1 , C_2 , and C_3 are given in the following paragraphs for vertical and horizontal surfaces. A surface can be considered vertical if the surface is less than 30° from the vertical; and a surface can be considered horizontal if it is less than 30° from the horizontal.

Vertical Surfaces

$C_1 = 0.59$, $C_2 = 0.25$, and $C_3 = 0.25$ for $G_r P_r < 10^9$ (laminar)

$C_1 = 0.10$, $C_2 = 0.333$, and $C_3 = 0.333$ for $G_r P_r > 10^9$ (turbulent)

Horizontal Surfaces

(1) Heated surfaces facing up or cooled surfaces facing down

$C_1 = 0.54$, $C_2 = 0.25$, and $C_3 = 0.25$ for $G_r P_r < 10^7$ (laminar)

$C_1 = 0.15$, $C_2 = 0.333$, and $C_3 = 0.333$ for $G_r P_r > 10^7$ (turbulent)

(2) Heated surfaces facing down or cooled surfaces facing up

$$C_1 = 0.27, C_2 = 0.25, \text{ and } C_3 = 0.25$$

For both FS877 and WS240, the gas temperatures were assumed equal to the ambient air temperatures (table 1). The wall temperatures for FS877 and WS240 were determined from the flight-measured temperatures obtained from thermocouple (TC) locations shown in figures 13 and 14 (Gong and others, 1987). Part of those flight data is shown in figures 9 and 10. The heat transfer coefficients h for C21 and C41 elements were then computed for profile times of 1700, 1800, 1900, 2000, 2400, and 3000 sec and are listed in table 2 for FS877 and table 3 for WS240. Heat transfer coefficients were not computed for times prior to time 1700 sec because the comparison between the measured and calculated structural temperatures showed that air ingestion did not affect structural temperatures until approximately 1700 sec.

RESULTS

Fuselage

Calculated time histories of the fuselage structural temperatures compared with flight-measured data are shown in figure 15. The dashed curves (taken from fig. 9 for 100 percent TPS thickness) are for the case when only the effect of internal convection was ignored. With the inclusion of internal free convection (solid curves), the structural temperature predictions were generally improved greatly. The predictions at stations on the bottom of the fuselage and at the glove region agree quite well with the measured data. The agreement between the measured and calculated temperatures at the two locations on the side of the fuselage (JLOC372 and JLOC384) shows only a relatively small improvement with the addition of free convection. The long and short broken curves in figure 15 are for the case when both internal convection and internal radiation were neglected. Without these two effects, the calculated peak fuselage structural temperatures at fuselage bottom could be as much as 50 to 90 percent higher than the measured data (at $t = 3000$ sec). Also, the magnitude of the internal convection is higher than that of internal radiation.

Wing

A comparison between measured and calculated structural temperatures for WS240 is shown in figure 16. The inclusion of free convection (solid curves) greatly improved the agreement between measured and calculated values. The agreement for the lower surfaces of bays 1, 2, and 3 and the agreement for all the upper surfaces are quite good. However, the calculated values for the lower surface of bay 4 are only in fair agreement with the measured data. This poorer agreement at bay 4 is probably due to the boundary conditions used in the analysis. It was assumed that the aft spar and web of bay 4 was perfectly insulated. In actuality, there was undoubtedly some heat loss that was not accounted for in the thermal model.

CONCLUSIONS

Finite-element heat transfer analysis was performed on the space shuttle orbiter fuselage and wing under STS-5 reentry heating. With the introduction of internal free convection effect in addition to conduction and internal radiation effects, the correlation between calculated and measured structural temperatures could be improved greatly. The effect of the internal convection was found to be larger than that of internal radiation. Without considering the

effects of both internal convection and internal radiation, the structural temperatures could be overpredicted by as much as 50 to 90 percent for the fuselage bottom skin and by 45 to 60 percent for the wing lower skin, respectively.

*Ames Research Center
Dryden Flight Research Facility
National Aeronautics and Space Administration
Edwards, California, February 5, 1988*

APPENDIX—THERMAL PROPERTIES OF SPACE SHUTTLE ORBITER MATERIALS

THERMAL PROPERTIES OF ALUMINUM ($\gamma = 175 \text{ lb/ft}^3$)

T , °F	k , Btu/ft-hr-°F	C_p , Btu/lb-°F
-420	13.0	---
-350	31.0	---
-300	39.0	---
-200	52.5	---
-100	61.5	---
0	69.0	---
75	---	0.206
100	74.0	---
200	78.0	0.215
300	82.0	0.222
400	84.7	0.228
500	87.0	0.234
600	89.4	---
800	92.0	---

THERMAL PROPERTIES OF ROOM TEMPERATURE VULCANIZED (RTV)

γ , lb/ft ³	k , Btu/ft-hr-°F	C_p , Btu/lb-°F
88	0.18	0.35

THERMAL PROPERTIES OF HIGH-TEMPERATURE
REUSABLE SURFACE INSULATION AND
LOW-TEMPERATURE REUSABLE SURFACE INSULATION
($\gamma = 9 \text{ lb/ft}^3$)

T, °F	k, Btu/ft-hr-°F					
	p, lb/ft ²					
	0	0.21	2.12	21.16	211.6	2116.0
-250	0.0050	0.0050	0.0075	0.0150	0.0216	0.0233
0	0.0075	0.0075	0.0100	0.0183	0.0250	0.0275
250	0.0092	0.0092	0.0125	0.0225	0.0316	0.0341
500	0.0125	0.0125	0.0167	0.0276	0.0400	0.0433
750	0.0175	0.0175	0.0216	0.0325	0.0492	0.0534
1000	0.0233	0.0233	0.0275	0.0392	0.0600	0.0658
1250	0.0308	0.0308	0.0350	0.0492	0.0725	0.0782
1500	0.0416	0.0416	0.0459	0.0617	0.0875	0.0942
1750	0.0567	0.0567	0.0610	0.0767	0.1060	0.1130
2000	0.0734	0.0734	0.0782	0.0942	0.1270	0.1360
2300	0.0966	0.0966	0.1020	0.1160	0.1550	0.1670
2500	0.1160	0.1160	0.1230	0.1390	0.1790	0.1940
2800	0.1540	0.1540	0.1620	0.1800	0.2220	0.2420
3000	0.1900	0.1900	0.1960	0.2190	0.2620	0.2900

T, °F	C _p , Btu/lb-°F
-250	0.070
-150	0.105
0	0.150
250	0.210
500	0.252
750	0.275
1000	0.288
1250	0.296
1700	0.302
1750	0.303
2300	0.303
3000	0.303

THERMAL PROPERTIES OF FELT REUSABLE SURFACE INSULATION

$$(\gamma = 5.4 \text{ lb/ft}^3)$$

T , °F	k , Btu/ft-hr-°F						
	p , lb/ft ²						
	0	0.021	0.212	2.116	21.16	211.6	2116.0
-250	0.0065	0.0065	0.0070	0.0080	0.0092	0.0102	0.0110
0	0.0080	0.0080	0.0105	0.0140	0.0171	0.0198	0.0206
100	0.0086	0.0086	0.0120	0.0166	0.0205	0.0238	0.0250
200	0.0095	0.0095	0.0138	0.0194	0.0240	0.0275	0.0290
300	0.0102	0.0102	0.0155	0.0222	0.0275	0.0322	0.0335
400	0.0110	0.0110	0.0170	0.0250	0.0316	0.0370	0.0382
600	0.0130	0.0130	0.0207	0.0315	0.0407	0.0475	0.0489
800	0.0150	0.0150	0.0250	0.0380	0.0500	0.0608	0.0620
1000	0.0175	0.0175	0.0300	0.0462	0.0615	0.0775	0.0795

T , °F	C_p , Btu/lb-°F
-250	0.300
0	0.312
200	0.320
400	0.335
600	0.345
800	0.360
1000	0.380

THERMAL PROPERTIES OF STRAIN ISOLATION PAD
 $(\gamma = 5.4 \text{ lb/ft}^3)$

T , °F	k , Btu/ft-hr-°F					
	p , lb/ft ²					
	0	0.2116	2.116	21.16	211.6	2116.0
-250	0.0048	0.0048	0.0080	0.0098	0.0103	0.0107
0	0.0053	0.0053	0.0110	0.0178	0.0198	0.0205
100	0.0057	0.0057	0.0124	0.0208	0.0235	0.0244
200	0.0063	0.0063	0.0135	0.0240	0.0273	0.0285
300	0.0073	0.0073	0.0152	0.0272	0.0318	0.0330
400	0.0091	0.0091	0.0168	0.0303	0.0371	0.0382
600	0.0120	0.0120	0.0205	0.0390	0.0480	0.0493
800	0.0156	0.0156	0.0250	0.0500	0.0608	0.0620
1000	0.0205	0.0205	0.0310	0.0620	0.0730	0.0750

T , °F	C_p , Btu/lb-°F
-100	0.140
0	0.190
100	0.258
200	0.344
300	0.450
400	0.575

THERMAL PROPERTIES OF
HIGH-TEMPERATURE REUSABLE
SURFACE INSULATION/
LOW-TEMPERATURE REUSABLE
SURFACE INSULATION
SURFACE COATING
($\gamma = 104 \text{ lb/ft}^3$)

T , °F	k , Btu/ft-hr-°F	C_p , Btu/lb-°F
-250	0.425	0.150
-150	0.450	0.170
0	0.487	0.190
250	0.550	0.215
500	0.604	0.240
750	0.654	0.260
1000	0.704	0.285
1250	0.750	0.300
1500	0.796	0.315
1700	0.829	0.325
1750	0.837	0.330
1950	0.871	0.340
2000	0.883	0.345
2100	0.896	0.350
2150	0.904	0.353
2300	0.933	0.360
2500	0.975	0.375
2800	1.080	0.390
3000	1.180	0.390

THERMAL PROPERTIES OF
GRAPHITE/EPOXY COMPOSITE
($\gamma = 98.4 \text{ lb/ft}^3$)

k , Btu/ft-hr-°F				
T , °F	Tape and fabric reinforcement		T , °F	C_p , Btu/lb-°F
	Parallel	Normal		
-290	0.58	0.15	-300	0.049
-150	1.19	0.23	-100	0.132
-50	1.51	0.28	100	0.208
100	1.96	0.36	300	0.277
200	2.14	0.39		
300 ^a	2.29	0.43		

^aExtrapolated.

RADIATION PROPERTIES

Region	ϵ	r
Windward TPS surface	0.85	0.15
Leeward TPS surface	0.80	0.20
Aluminum surface	0.667	0.333
Space	1.0	0.0

REFERENCES

- Gong, Leslie, William L. Ko, and Robert D. Quinn, *Thermal Response of Space Shuttle Wing During Reentry Heating*, AIAA 84-1761, June 1984. (Also published as NASA TM-85907, 1984.)
- Gong, Leslie, William L. Ko, and Robert D. Quinn, *Comparison of Flight-Measured and Calculated Temperatures on Space Shuttle Orbiter*, NASA TM-88278, 1987.
- Gong, Leslie, Robert D. Quinn, and William L. Ko, *Reentry Heating Analysis of Space Shuttle With Comparison of Flight Data*, NASA CP-2216, 1982, pp. 271-294.
- Ko, William L., Robert D. Quinn, Leslie Gong, Lawrence S. Schuster, and David Gonzales, *Preflight Reentry Heat Transfer Analysis of Space Shuttle*, AIAA 81-2382, Nov. 1981.
- Ko, William L., Robert D. Quinn, Leslie Gong, Lawrence S. Schuster, and David Gonzales, *Reentry Heat Transfer Analysis of the Space Shuttle Orbiter*, NASA CP-2216, 1982, pp. 295-325.
- Ko, William L., Robert D. Quinn, and Leslie Gong, *Finite-Element Reentry Heat Transfer Analysis of Space Shuttle Orbiter*, NASA TP-2657, 1986.
- Marlowe, M.B., R.A. Moore, and W.D. Whetstone, *SPAR Thermal Analysis Processors Reference Manual, System Level 16*, NASA CR-159162, 1979.

TABLE 1. AMBIENT AIR
TEMPERATURES (LISTED FOR
FREE CONVECTION EXCHANGE
TEMPERATURES)

Time, sec	Convection exchange temperature T , °F
1700	-3.77
1750	28.82
1800	57.93
1820 ^a	57.93
1900	57.93
2000	57.93
2400	57.93
3000	57.93

^aTouchdown.

TABLE 2. HEAT TRANSFER COEFFICIENTS CALCULATED
FOR INTERNAL FREE CONVECTION INSIDE FS877

Convective			
surface ID	JLOC, TC ^a	Time, sec	$h, \frac{\text{Btu}}{\text{in.}^2 \cdot \text{sec} \cdot ^\circ\text{F}} \times 10^{-6}$
1	24 VO9T9525	1700	1.80
		1800	2.30
		1900	2.30
		2000	2.20
		2400	2.10
		3000	1.90
2	108 VO9T9506	1700	1.90
		1800	2.40
		1900	2.40
		2000	2.30
		2400	2.00
		3000	1.70
3	132 VO9T9707	1700	1.70
		1800	2.00
		1900	2.00
		2000	2.00
		2400	1.80
		3000	1.60
4	192 VO9T9206	1700	1.48
		1800	1.60
		1900	1.62
		2000	1.60
		2400	1.78
		3000	1.78

TABLE 2. Concluded.

Convective			
surface	JLOC,	Time,	$h, \frac{\text{Btu}}{\text{in.}^2 \cdot \text{sec} \cdot ^\circ\text{F}} \times 10^{-6}$
ID	TC ^a	sec	
5	300 VO9T9157	1700	0.85
		1800	0.72
		1900	0.72
		2000	0.72
		2400	0.72
		3000	0.72
6	372 VO9T9377	1700	1.10
		1800	1.20
		1900	1.10
		2000	1.00
		2400	0.80
		3000	0.40
7	384 VO9T9501	1700	0.90
		1800	0.00
		1900	0.00
		2000	0.00
		2400	0.00
		3000	0.00
8	312 VO9T9708	1700	0.81
		1800	0.41
		1900	0.41
		2000	0.41
		2400	0.41
		3000	0.88
9	530 VO9T9709	1700	0.81
		1800	0.41
		1900	0.41
		2000	0.41
		2400	0.41
		3000	0.88

^aJLOC = joint location (or node), TC = thermocouple.

**TABLE 3. HEAT TRANSFER COEFFICIENTS
CALCULATED FOR INTERNAL FREE
CONVECTION INSIDE WS240**

Surface ID	Time, sec	$h, \frac{\text{Btu}}{\text{in.}^2 \cdot \text{sec} \cdot ^\circ\text{F}} \times 10^{-6}$
1	1700	1.41
	1800	1.64
	1900	1.77
	2000	1.85
	2200	1.93
	2400	1.93
	3000	1.78
2	1700	0.46
	1800	1.10
	1900	1.12
	2000	1.11
	2200	1.04
	2400	0.97
	3000	0.63
3	1700	0.76
	1800	0.76
	1900	0.70
	2000	0.49
	2200	0.46
	2400	0.63
	3000	0.63
4	1700	0.32
	1800	0.35
	1900	0.33
	2000	0.31
	2200	0.30
	2400	0.30
	3000	0.30

TABLE 3. Continued.

Surface ID	Time, sec	$h, \frac{\text{Btu}}{\text{in.}^2 \cdot \text{sec} \cdot ^\circ\text{F}} \times 10^{-6}$
5	1700	1.43
	1800	1.68
	1900	1.79
	2000	1.85
	2200	1.85
	2400	1.83
	3000	1.61
6	1700	0.74
	1800	0.86
	1900	0.77
	2000	0.64
	2200	0.32
	2400	0.57
	3000	0.70
7	1700	0.32
	1800	0.19
	1900	0.19
	2000	0.19
	2200	0.22
	2400	0.26
	3000	0.29
8	1700	1.44
	1800	1.69
	1900	1.79
	2000	1.81
	2200	1.80
	2400	1.74
	3000	1.59
9	1700	0.74
	1800	0.81
	1900	0.70
	2000	0.53
	2200	0.32
	2400	0.25
	3000	0.29

TABLE 3. Concluded.

Surface ID	Time, sec	$h, \frac{\text{Btu}}{\text{in.}^2 \cdot \text{sec} \cdot ^\circ\text{F}} \times 10^{-6}$
10	1700	0.30
	1800	0.30
	1900	0.27
	2000	0.22
	2200	0.22
	2400	0.22
	3000	0.22
11	1700	1.49
	1800	1.88
	1900	1.93
	2000	1.93
	2200	1.90
	2400	1.96
	3000	1.61
12	1700	0.73
	1800	0.98
	1900	0.93
	2000	0.85
	2200	0.69
	2400	0.50
	3000	0.58
13	1700	0.30
	1800	0.24
	1900	0.22
	2000	0.22
	2200	0.22
	2400	0.22
	3000	0.22

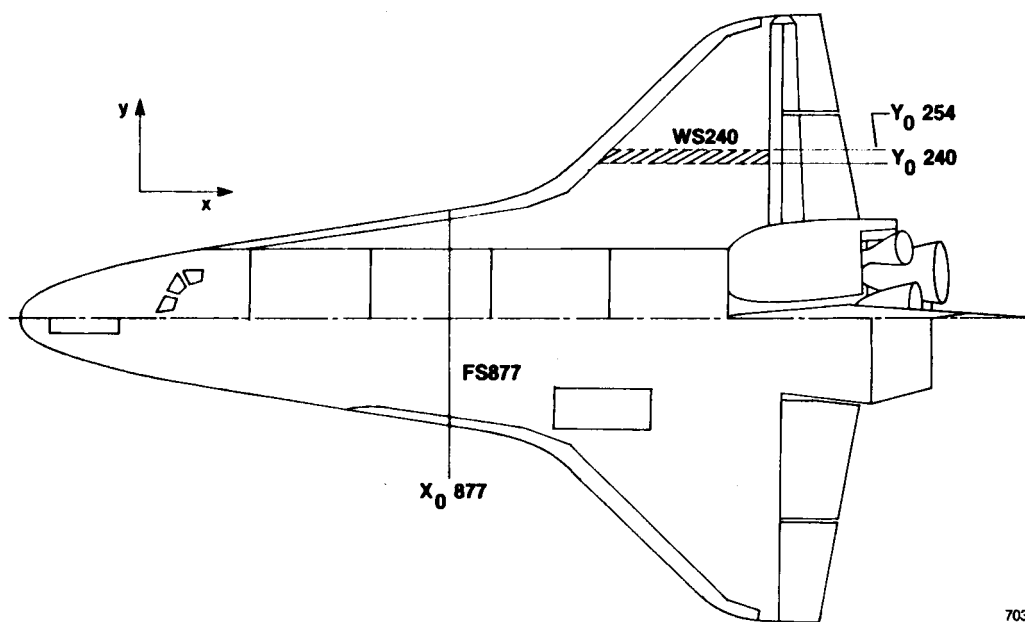


Figure 1. Locations of space shuttle orbiter structures analyzed.

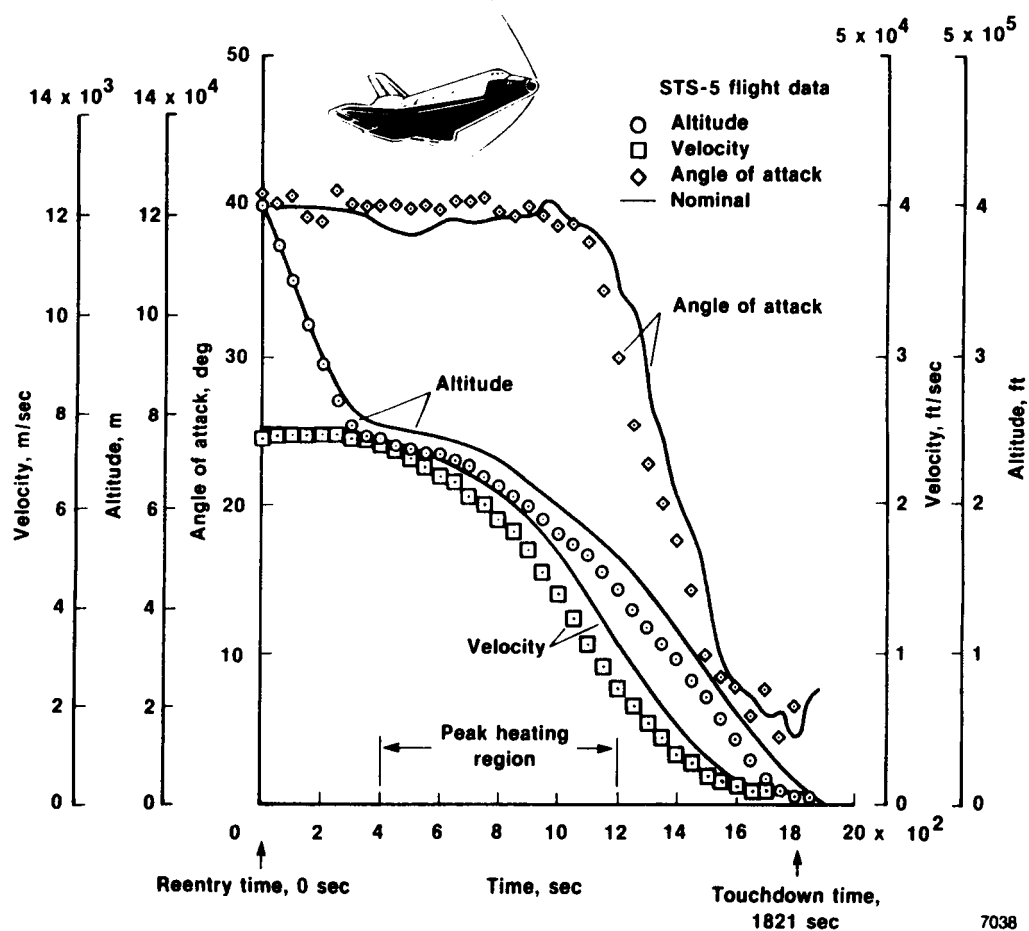


Figure 2. Reentry trajectory for STS-5.

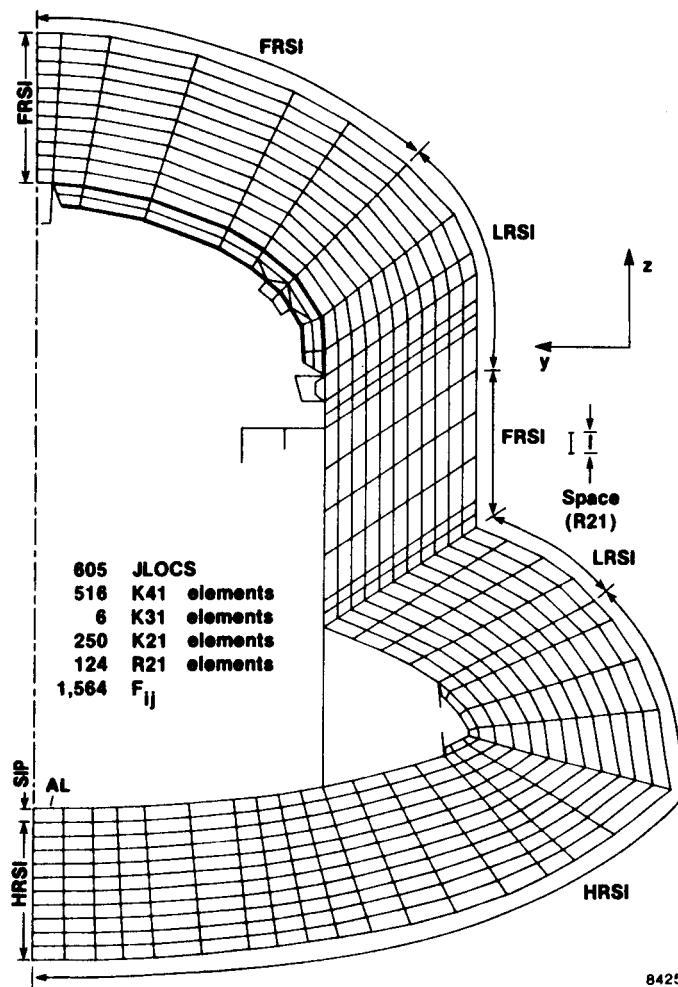


Figure 3. Thermal model setup for FS877. No convection elements (Ko and others, 1986).

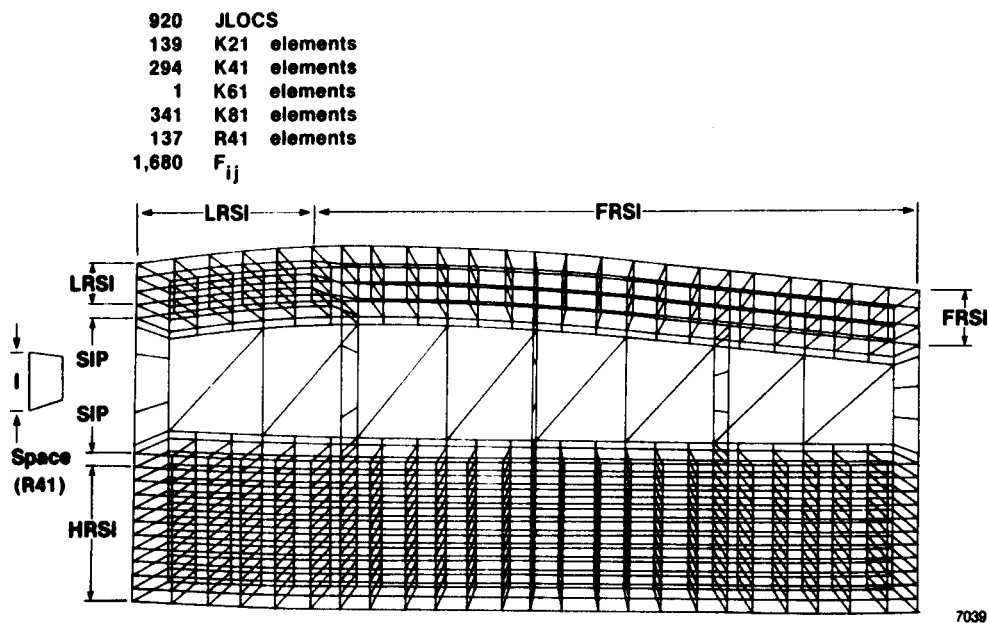


Figure 4. Thermal model setup for WS240. No convection elements (Ko and others, 1986).

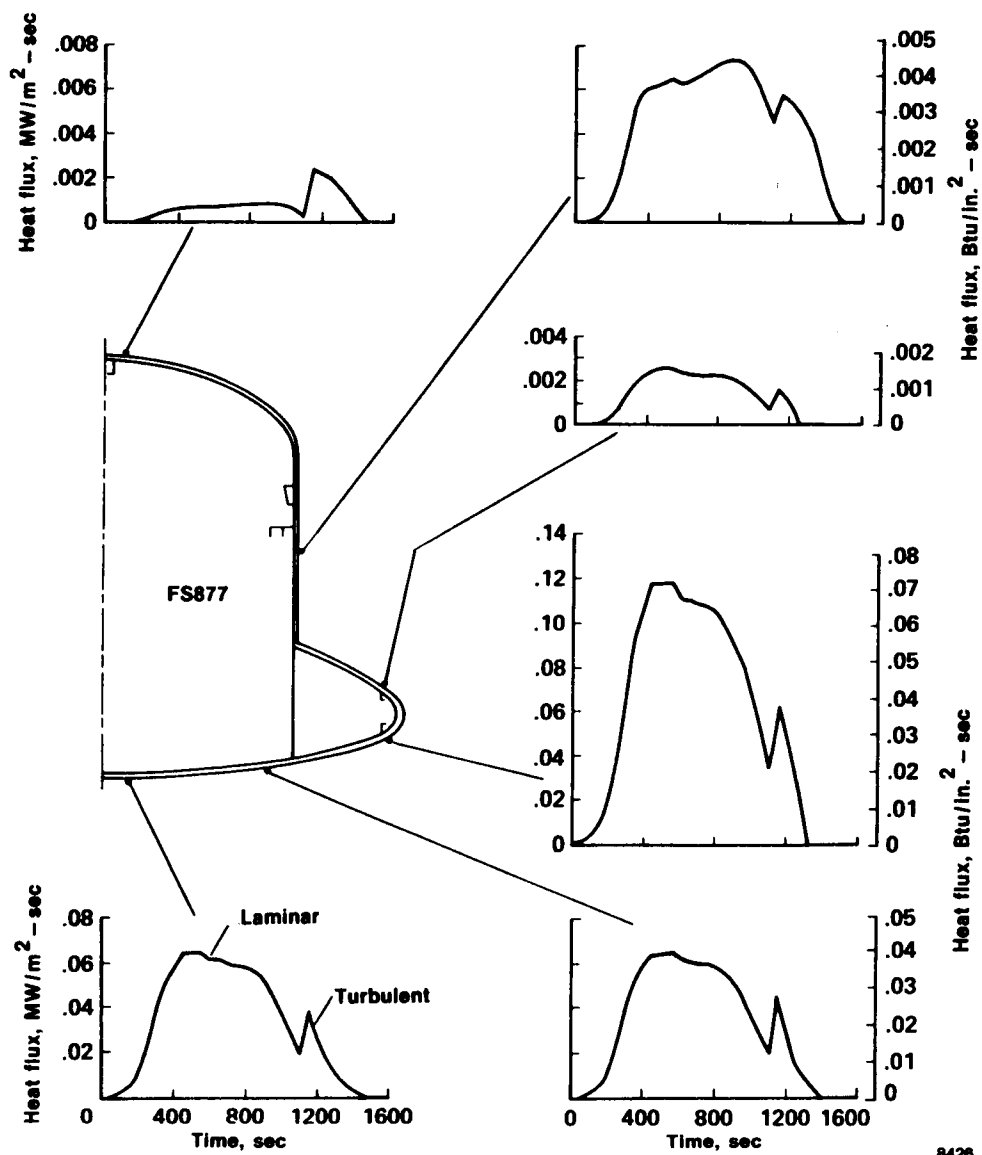


Figure 5. Surface heating rates for FS877 calculated from STS-5 flight trajectory (Ko and others, 1986).

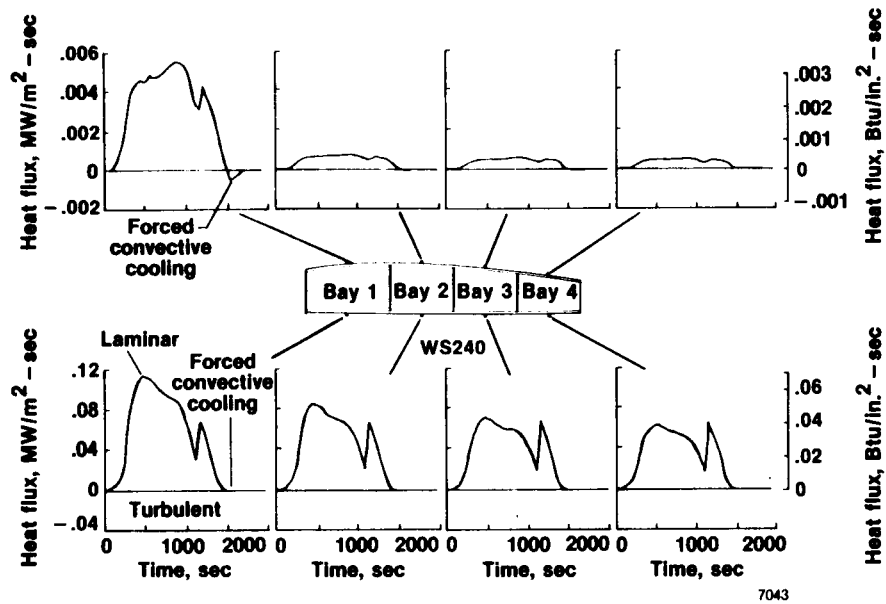


Figure 6. Surface heating rates for WS240 calculated from STS-5 flight trajectory (Ko and others, 1987).

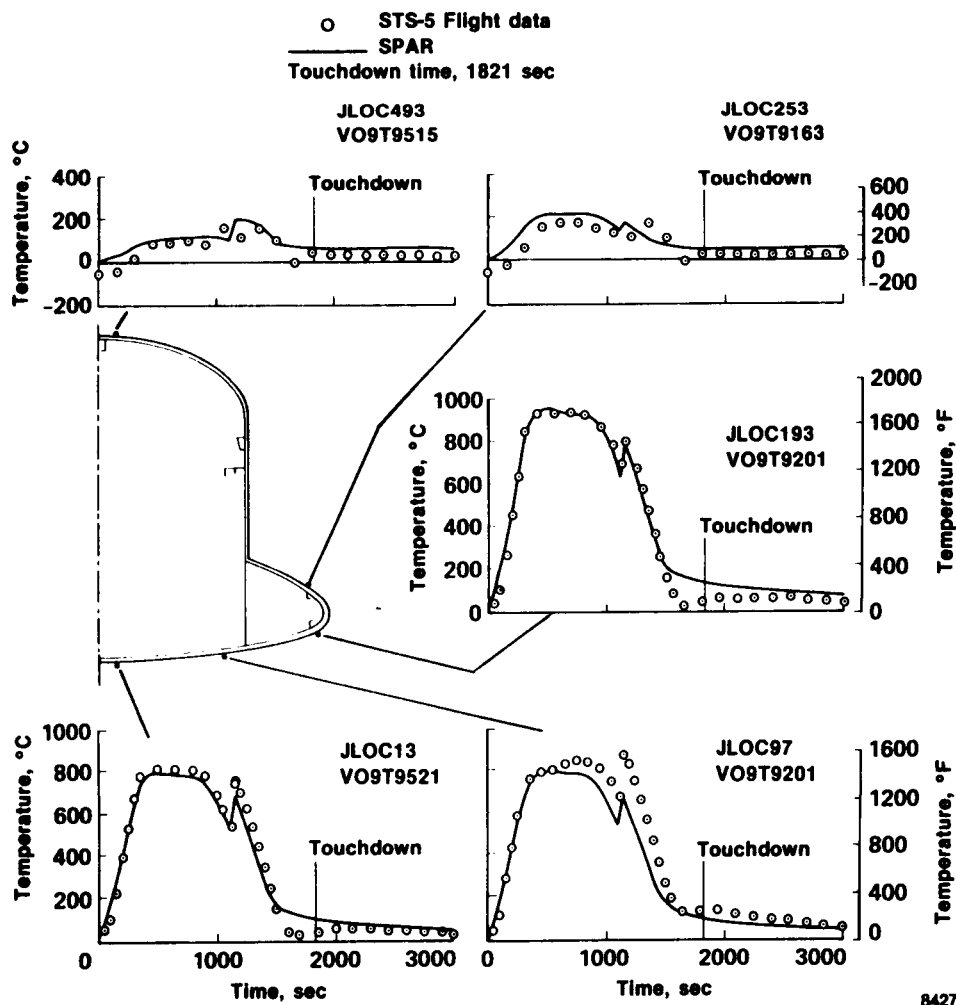


Figure 7. Time histories of thermal protection system surface temperatures of FS877, STS-5 flight (Ko and others, 1986).

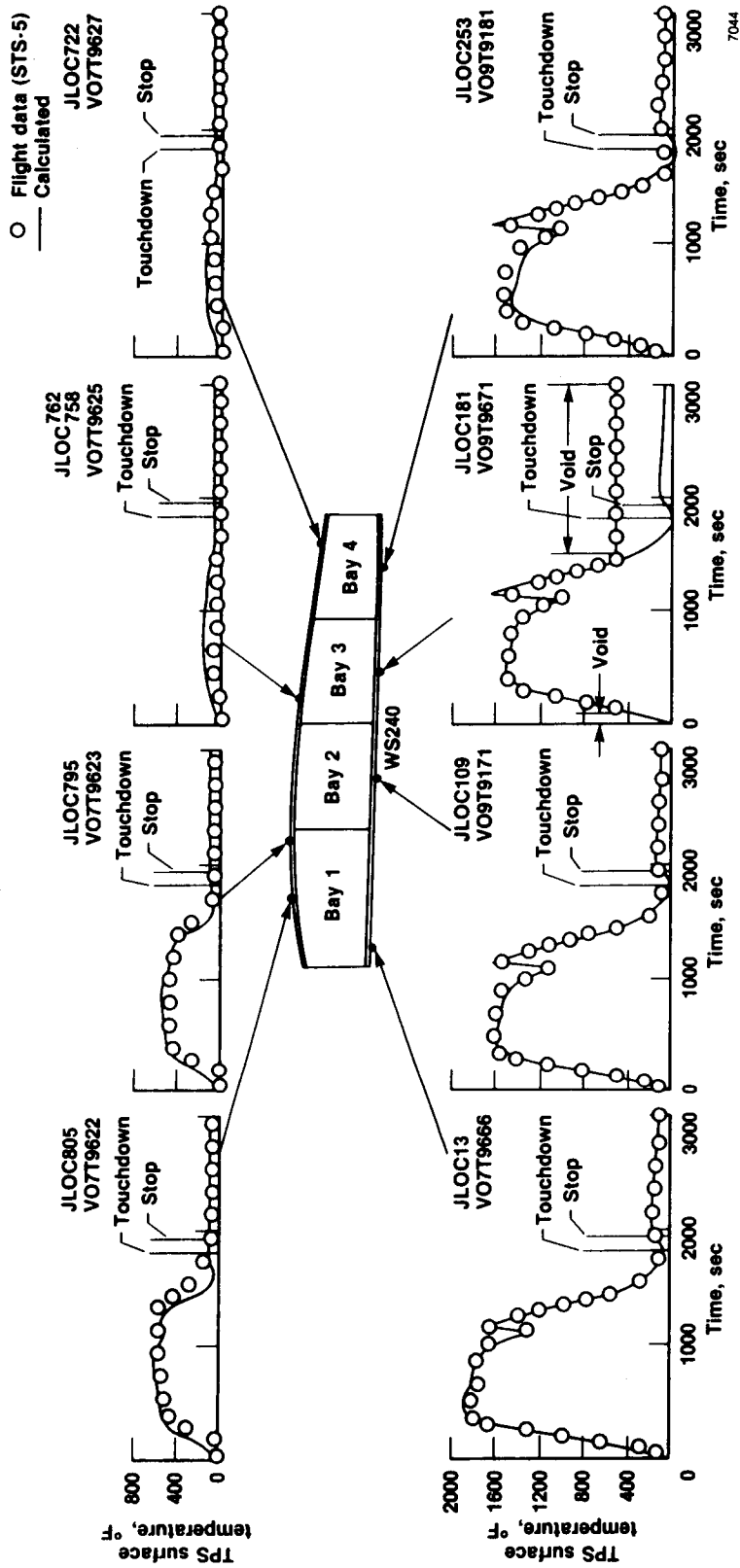
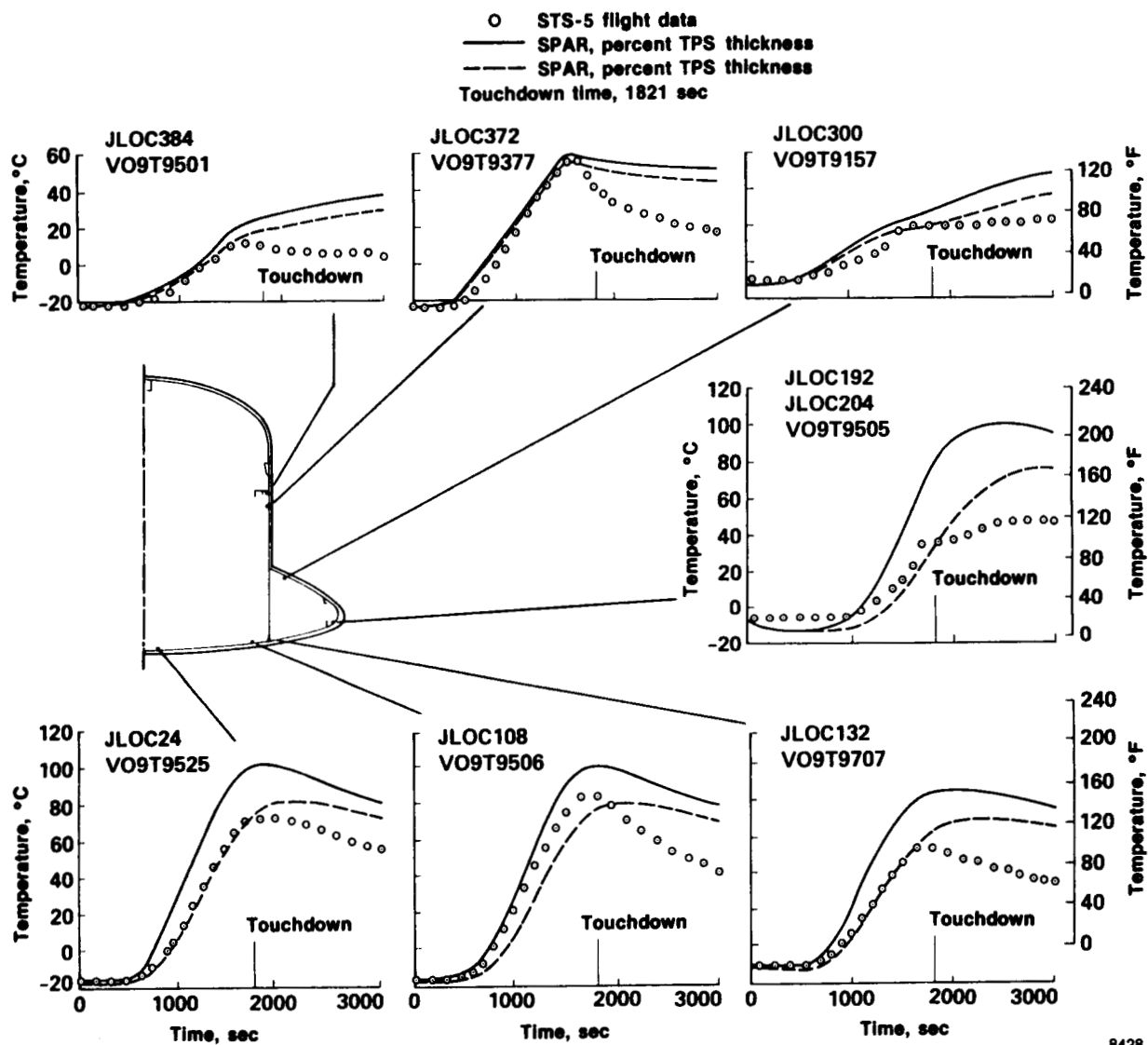
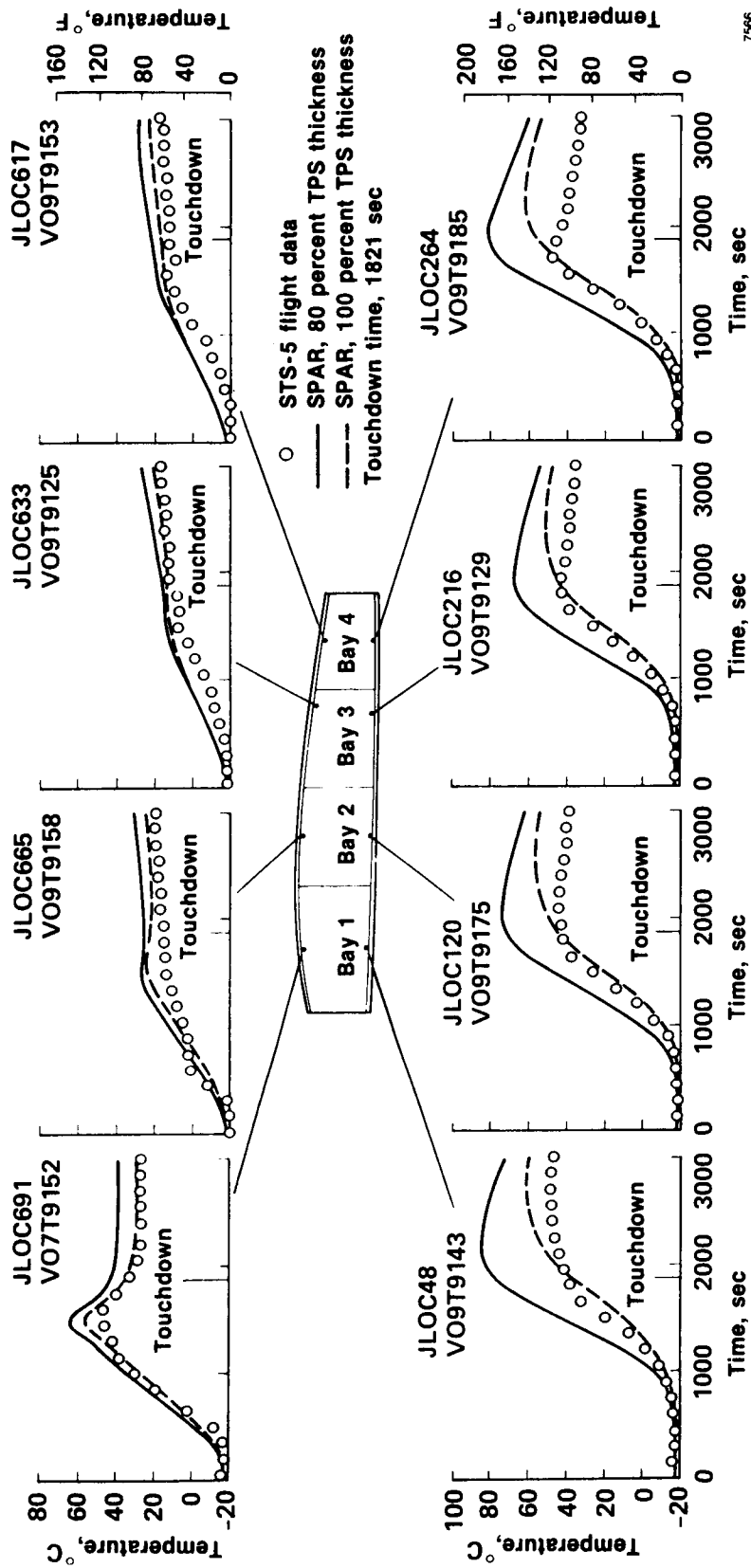


Figure 8. Time histories of thermal protection system surface temperatures of WS240, STS-5 flight (Ko and others, 1987).



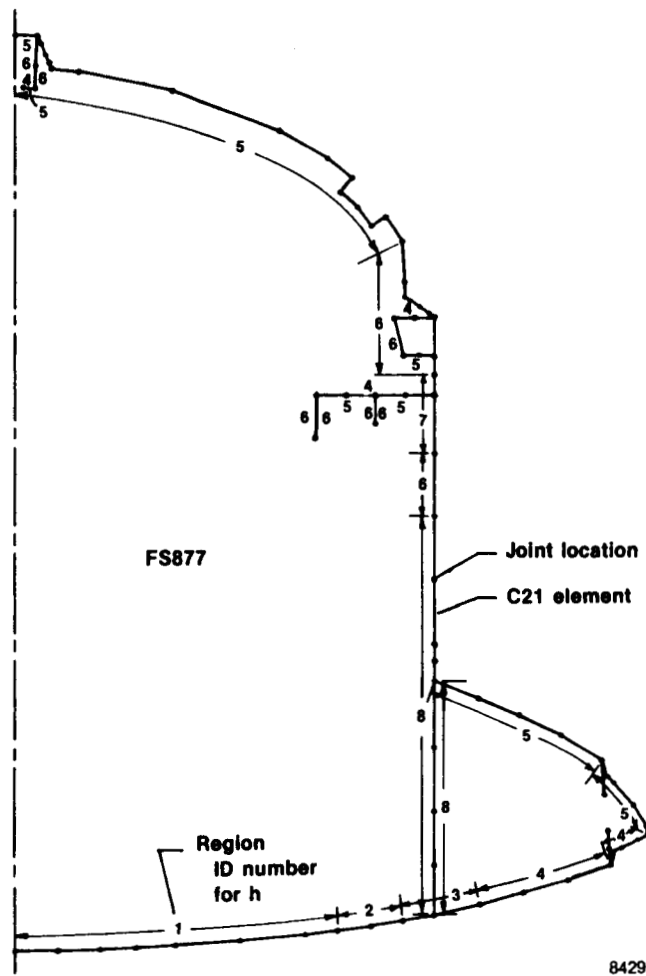
8428

Figure 9. Time histories of structural temperatures of FS877. Internal convection neglected, STS-5 flight (Ko and others, 1986).



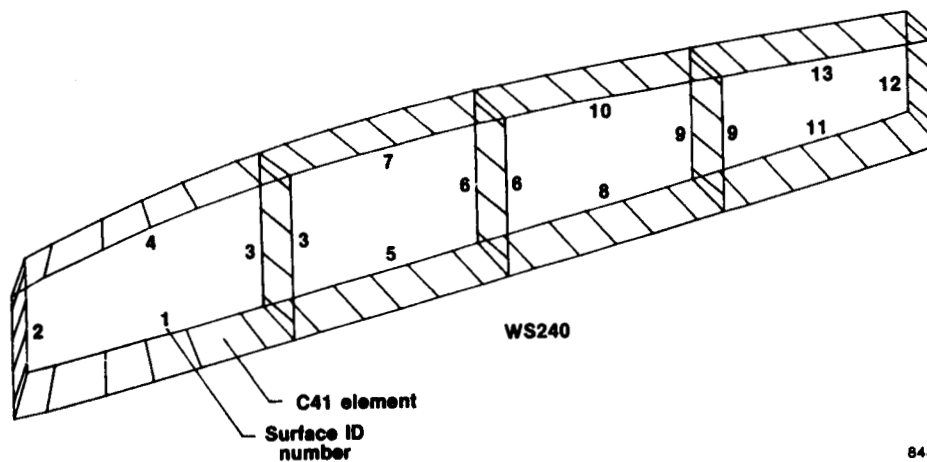
7566

Figure 10. Time histories of structural temperatures for WS240. Internal convection neglected, STS-5 flight (Ko and others, 1986).



8429

Figure 11. A total of 96 C21 elements added to the existing thermal model FS877 shown in figure 3 for modeling internal free convection. Small numerals indicate regions for different h .



8430

Figure 12. A total of 88 C41 elements attached to bay cavities of WS240 to model internal free convection.

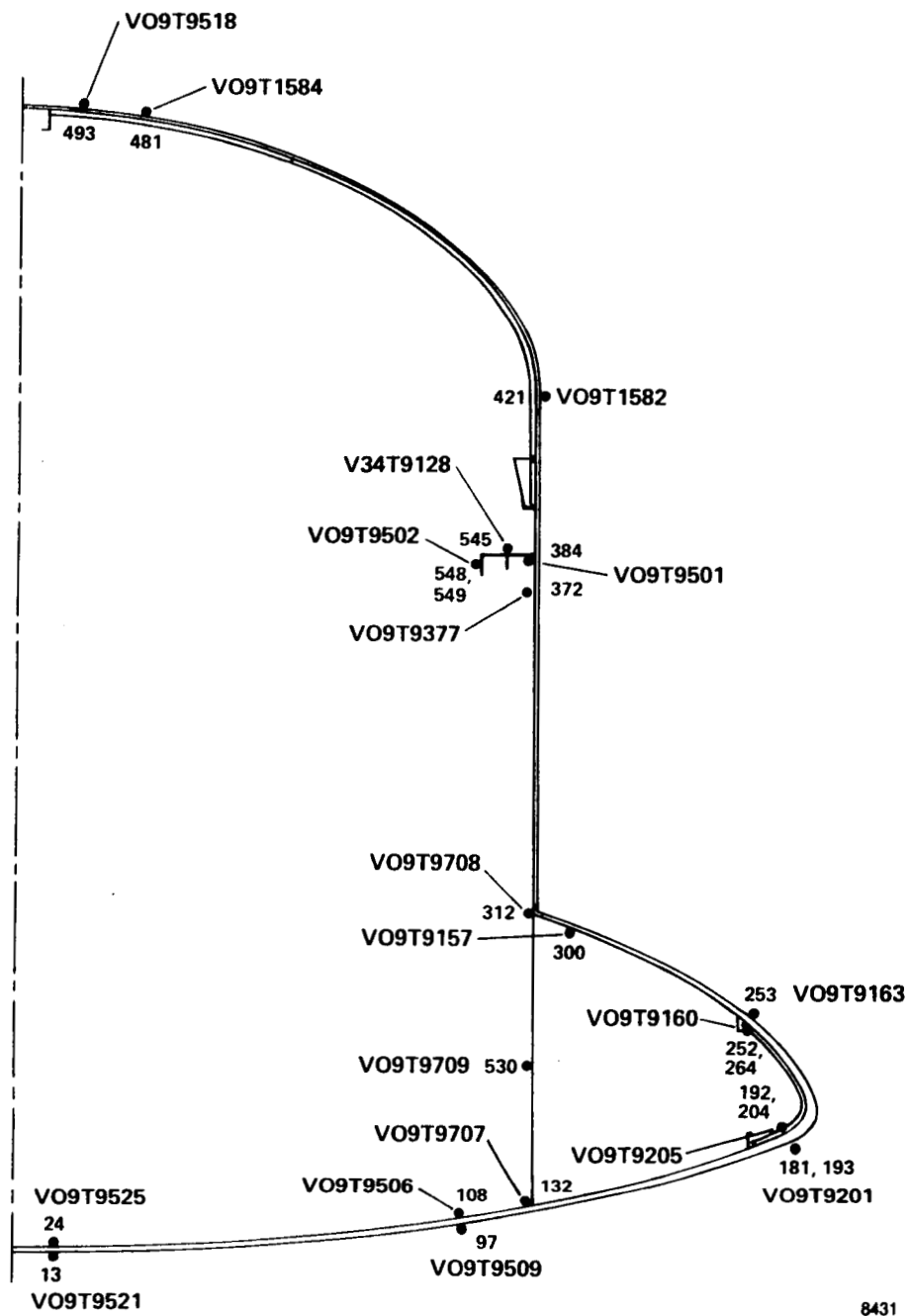


Figure 13. Thermocouple locations on FS877. Small numerals indicate joint location (or node) numbers (Ko and others, 1986).



Figure 14. Thermocouple locations on WS240. Small numerals indicate joint location (or node) numbers (Ko and others, 1986).

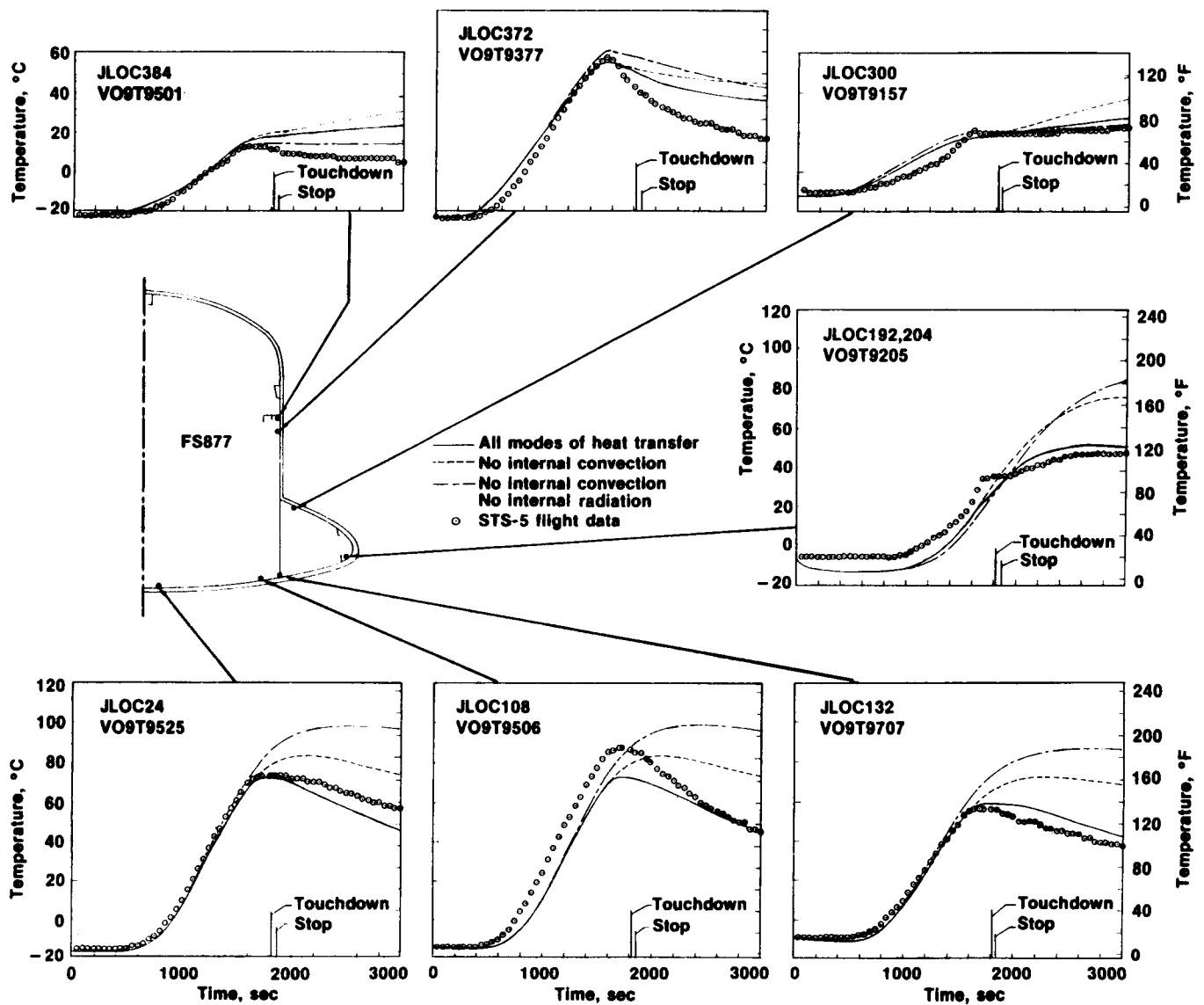


Figure 15. Time histories of structural temperatures of FS877, STS-5 flight.

8433

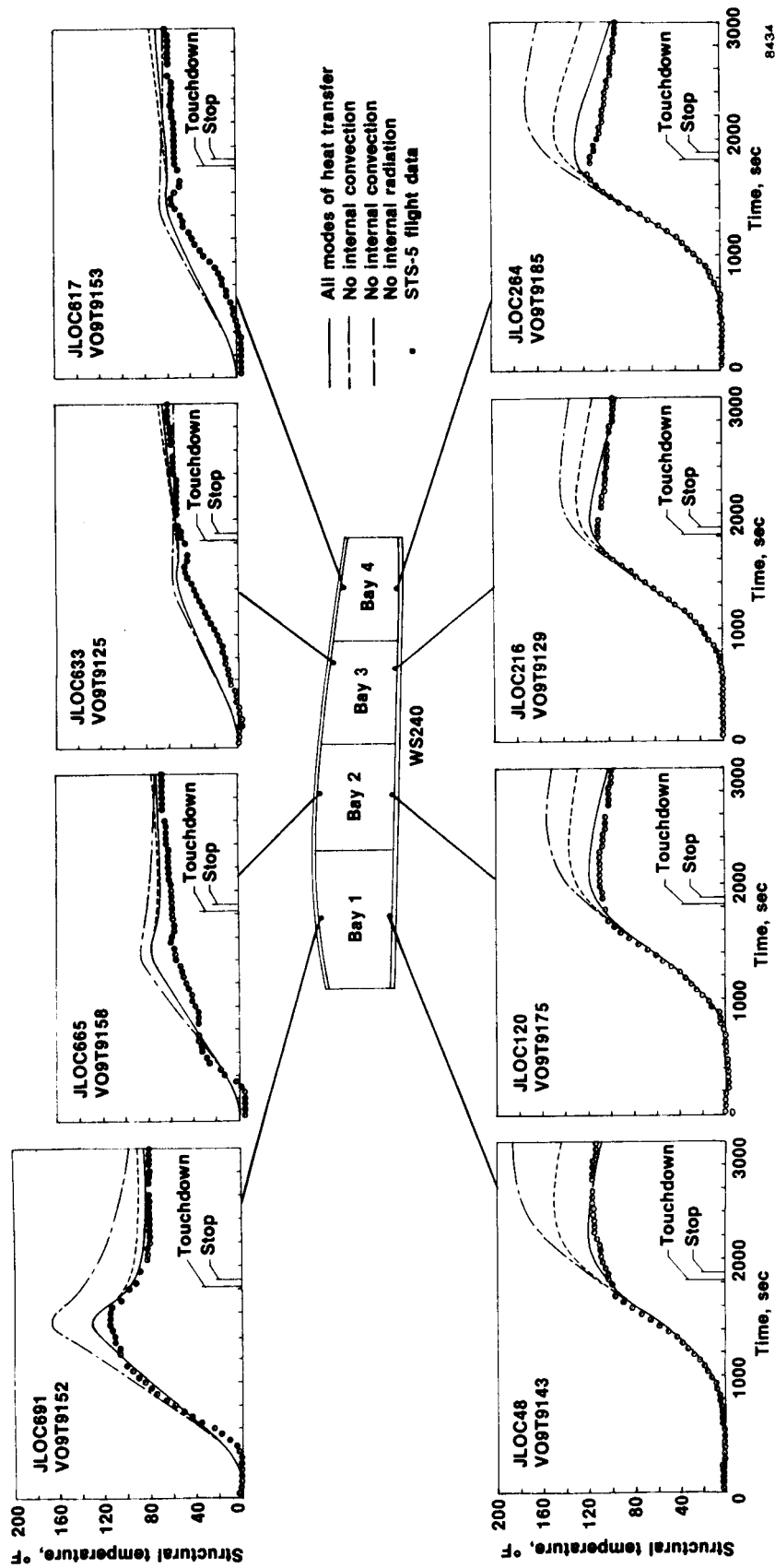


Figure 16. Time histories of structural temperatures of WS240, STS-5 flight.



Report Documentation Page

1. Report No. NASA TM- 100414		2. Government Accession No.		3. Recipient's Catalog No.	
4. Title and Subtitle Effect of Internal Convection and Internal Radiation on the Structural Temperatures of Space Shuttle Orbiter				5. Report Date October 1988	
				6. Performing Organization Code	
7. Author(s) William L. Ko, Robert D. Quinn, and Leslie Gong				8. Performing Organization Report No. H-1466	
				10. Work Unit No. RTOP 532-09-01	
9. Performing Organization Name and Address NASA Ames Research Center Dryden Flight Research Facility P.O. Box 273, Edwards, CA 93523-5000				11. Contract or Grant No.	
				13. Type of Report and Period Covered Technical Memorandum	
12. Sponsoring Agency Name and Address National Aeronautics and Space Administration Washington, DC 20546				14. Sponsoring Agency Code	
15. Supplementary Notes					
16. Abstract Structural performance and resizing (SPAR) of the finite-element thermal analysis computer program was used in the reentry heat transfer analysis of the space shuttle orbiter. One midfuselage cross section and one midspan wing segment were selected to study the effects of internal convection and internal radiation on the structural temperatures. The effect of internal convection was found to be more prominent than that of internal radiation in the orbiter thermal analysis. Without these two effects, the calculated structural temperatures at certain stations could be as much as 45 to 90 percent higher than the measured values. By considering internal convection as free convection, the correlation between the predicted and measured structural temperatures could be improved greatly.					
17. Key Words (Suggested by Author(s)) Internal convection Internal radiation Space shuttle orbiter Structural temperatures			18. Distribution Statement Unclassified — Unlimited Subject category 34		
19. Security Classif. (of this report) Unclassified	20. Security Classif. (of this page) Unclassified	21. No. of pages 34	22. Price A03		